Pergamon

Nucl. Tracks Radiat. Meas., Vol. 21, No. 4, pp. 543–554, 1993

0969-8078/93 $6.00 + .00

THERMAL AND UNROOFING HISTORY OF THE LHASA AREA, SOUTHERN TIBET—EVIDENCE FROM APATITE FISSION TRACK THERMOCHRONOLOGY

YUN PAN,* PETER COPELAND,† MARY K. RODEN,*‡ W. S. F. KIDD* and T. MARK HARRISON§

*Department of Geological Sciences, State University of New York at Albany, NY 12222, U.S.A.; †Department of Geology, University of Houston Central Campus, TX 77004, U.S.A.; ‡Department of Geology and Environmental Sciences, Rensselaer Polytechnic Institute, NY 12180-3590, U.S.A.; and §Department of Earth and Space Sciences, University of California at Los Angeles, CA 90024, U.S.A.

(*Received* 18 *September* 1992; *in revised form* 6 *August* 1993)

Abstract—New fission track (FT) thermochronologic data from plutonic rocks at the Gangdese magmatic arc support the view that there was a pulse of rapid cooling (>80°C/m.y.) and unroofing (>2 mm/m.y.) around 20–15 Ma in the Quxu area, southern Lhasa terrane. The average cooling rate prior to 20 Ma and post to 15 Ma was only about 5–6°C/m.y. in this area. A fast cooling and unroofing event was not detected in other studied areas in the Lhasa terrane. Average cooling rates of 4–10°C/m.y. since the India–Asia continental collision (45–0 Ma) and unroofing rates of 0.1–0.3 mm/y can be deduced for these areas from the fission track data and previously reported $^{40}Ar/^{39}Ar$ data. These relatively slow unroofing rates can be viewed as a regional "background" in this mountain-building area, and the rapid unroofing recorded in the Quxu area as a "pulse" superimposed on it. Apatites from the granitic gneisses of the Nyainqentanglha range, west of the Yangbajain graben, yield exceptionally young FT ages of 3.3–5.1 Ma. These ages together with $^{40}Ar/^{39}Ar$ data, allow cooling rates of 20 to ~200°C/m.y. (9–0 Ma) to be deduced at several locations. These young ages and fast cooling rates are interpreted to be the result of recent rapid uplift and exhumation of the foot-wall of a major normal-faulting detachment zone accompanying the Yangbajain graben.

1. INTRODUCTION

IT HAS been widely accepted that the Cenozoic continental collision between India and Asia was responsible for the crustal thickening and surface uplift of the Tibetan Plateau and the Himalayan Mountains (e.g. Dewey and Burke, 1973; Molnar and Tapponnier, 1975; Allègre *et al.*, 1984). However, the exact mechanism of crustal thickening and plateau building is still unknown. Several hypotheses have been proposed and they can be divided into two classes.

The first class of hypotheses assumes that the Indian plate has acted as a passive indenter. Tibetan crust has been shortened across its whole area by northward pushing of this indenter since the Indian continent started to collide with the Asian continent. Shortening occurred in the upper crustal levels by folding and thrusting as well as bulk straining, and at the lower crustal levels by ductile flow (Dewey and Burke, 1973; Dewey *et al.*, 1988). The crustal thickness of Tibet increased as the north–south length of Tibet decreased. This thickening process may or may not be accompanied by the lateral continental extrusion, which was proposed by Tapponnier and his co-workers (e.g. Tapponnier *et al.*, 1986). A further suggestion (England and Houseman, 1988) invokes an additional mechanism in order to explain the high altitude of Tibet. As a result of the thermal instability of the thickened lithosphere, a portion of the thickened lower Tibetan lithosphere catastrophically delaminated from its upper part, and hotter asthenosphere was then driven in between the two parts, causing rapid uplift because of isostatic compensation.

The second class of hypotheses includes the so-called continental subduction or underplating, and hydraulic injection models. In these models Indian continental material is thrust underneath Tibet, either by continental underthrusting, underplating (e.g. Powell and Conaghan, 1975; Powell, 1986), or by hydraulic injection (Zhao and Morgan, 1987). This class of hypotheses differs from the first one in that the Indian continental crust plays a role in the present Tibetan plateau: a large portion (~1000 km) of Indian continental crust was subducted or underplated beneath, or injected into the lower Tibetan crust.

Contrasting patterns of uplift as well as crustal thickening are predictable for the areas immediately north of the suture zone by the different tectonic hypotheses. Uplift and thickening of such areas would have been continuous and steady in the underplating, or fluid injection hypothesis, and may have

been steady in the distributed shortening hypothesis if lateral extrusion was negligible. Alternatively, in the case of simple underthrusting, uplift and crustal thickening would have been extremely rapid and would have occurred right after the initial collision. In the case of catastrophic delamination, uplift and thickening would have been initially slow followed by a dramatic increase at the time of delamination. Uplift and crustal thickening would have been episodic if thickening and lateral extrusion alternatively took place and if the latter absorbed sufficient collisional convergence. Thus, understanding the uplift and crustal thickening history is important in order to evaluate these hypotheses.

Under proper assumptions, thermochronological data may provide useful insights into this problem by revealing the thermal and unroofing history of rocks. Using $^{40}Ar/^{39}Ar$ data, Copeland *et al.* (1987) documented a pulse of exhumation between 20–17 Ma within the Quxu–Lhasa region of the Gangdese batholith. In this paper we present results of apatite FT analysis from the Lhasa area, including the Quxu–Lhasa region of Copeland *et al.* (1987). A generalized cooling and unroofing history is constructed, and the conclusion reached by Copeland *et al.* (1987) is supported by these new thermochronologic data. The implication of the unroofing history to the above tectonic problem is discussed.

2. GENERAL SETTING

A simplified geologic map of the Lhasa area is shown in Fig. 1. There is a continuous sedimentary sequence from Carboniferous to Cretaceous. The Upper Cretaceous clastic rocks (Takena Formation) are unconformably overlain by the widespread early Cenozoic volcanics with interbedded red beds (Linzizong Formation). Quaternary deposits are found mostly within the fault-bounded Yangbajain graben.

The Indus–Zangbo Suture (IZS) is the tectonically southern limit of the Lhasa Terrane and the Tibetan Plateau. In the area south of Lhasa the suture is marked by a belt of ophiolite outcrops along the Zangbo river. There are several lines of evidence indicating that the initial collision between Indian and Asian continents or the final closure of Neo-Tethyan was around 40–45 Ma along this suture (see Dewey *et al.*, 1988 for a discussion).

The Gangdese magmatic belt consists of the Gangdese batholith (sometimes referred to as the Trans-Himalaya batholith) and associated Genozoic volcanics. In southern Tibet, this belt is 2500 km long and 80–90 km wide forming the east trending Gangdese Shan mountain range, and it lies immediately north of the Indus–Zangbo Suture. The Gangdese batholith is composed predominantly of calc–alkaline rocks, with the common rock types being granite, granodiorite, diorite, tonalite, and

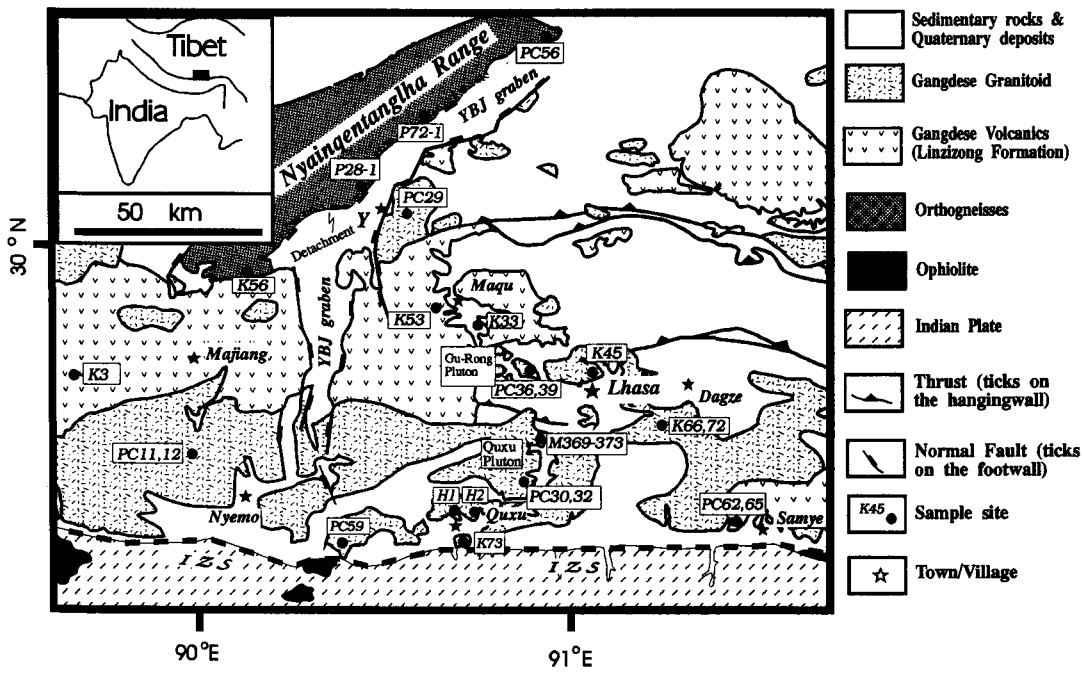

FIG. 1. Simplified geologic map of the Lhasa area, southern Tibet (after Kidd *et al.*, 1988), showing major structures, rock distributions, and sampling locations for this study. The dashed pattern at the southeastern margin of the Nyainqentanglha Range represents a major low-angle ductile detachment, dipping southeast toward the Yangbajain (YBJ) graben. The locations of the Quxu pluton and the Gu-Rong pluton are indicated on the map. IZS = Indus–Zangbo Suture.

some gabbro. The associated volcanics of the Linzizong Formation have similar composition and consist of rhyolitic to andesitic lava and tuff, as well as some basalt. It is believed that this belt was an Andean-type magmatic arc produced by the subduction of the Tethyan ocean floor of the Indian plate along the Zangbo suture zone (e.g. Gansser, 1981; Allègre *et al.*, 1984). Crystallization ages of between 110 and 40 Ma are reported for plutons of the Gangdese batholith in the Lhasa area, and the main episode of intrusion occurred around 60–40 Ma (Schärer *et al.*, 1984; Xu R.-H. *et al.*, 1985; Debon *et al.*, 1986). The volcanics exposed along the northern part of the Gangdese mountain range have eruption ages of 50–60 Ma, but there are also minor amounts of Miocene volcanics to the west of Yangbajain (Coulon *et al.*, 1986; Pan, 1993).

In the Nyainqentanglha area granitic orthogneisses of upper amphibolite facies crop out along the southwest and central part of the range. The peak metamorphic conditions were reported to be 700°C and 5 kb (Harris *et al.*, 1988), and these rocks are thought to have been brought to the surface from depths greater than 10 km. Xu *et al.* (1985) have reported zircon U–Pb ages of around 50 Ma from the granitic gneisses. A major shear zone in the Nyainqentanglha orthogneisses along the southeast margin of the range bounds the NE trending Yangbajain graben to the SE (see Fig. 1), and it has been interpreted as a major low-angle extensional detachment representing early extension in this area (Pan and Kidd, 1992).

3. FISSION TRACK RESULTS AND INTERPRETATION

Twenty-eight apatites from 18 locations (Fig. 1) in the Lhasa area of the Gangdese belt, most of them from granitic rocks and some from orthogneisses and volcanics, were analyzed in this study. Sample preparation procedures for age measurements using the external detector method (EDM) paralleled those of Green (1986). Irradiation with thermal-neutrons was done at the Oregon State University TRIGA reactor. Ages were calculated using a weighted mean zeta calibration factor (Hurford and Green, 1983) for CN1 glass dosimeter, determined by measuring spontaneous track densities in the Fish Canyon Tuff, Mount Dromedary and Durango standard apatites. Errors of FT ages were calculated according to Green (1981). The age measurements were done at the fission track lab at the Rensselaer Polytechnic Institute, using a Leitz Ortholux microscope with a 1600 × magnification (160 × dry objective, 10 × oculars). Confined track length measurements were done at 1563 × (100 × dry objective, 1.25 × tube, 12.5 × oculars) using a drawing tube and a Houston Instruments 1011 digitizing pad interfaced with an IBM PC XT computer. Most of the track length measurements were made in the conventional method, in which the confined tracks were revealed by the 5 M HNO_3 etchant that passed through cracks, cleavages, or surface-intersecting tracks. Confined track length measurements in samples K66 and K72 were made by M. K. Roden by using the ^{252}Cf technique. These two samples were placed in an evacuated chamber at ~8.9 cm from a ^{252}Cf source and irradiated for 18 h prior to etching and track length measurement. This technique allowed bombardment of the grain surfaces with ^{252}Cf fission fragments, thus producing pathways for the etchant to reach confined tracks within the grains. Without this irradiation, measurement of confined track lengths in these samples would have been impossible. Calibrations using standards of published mean track length were carried out between different workers within the lab.

An apatite FT age with a simple cooling history has been generally interpreted as the time the rock cooled through ~100°C (Wagner, 1968; Naeser and Faul, 1969; Naeser, 1981; Gleadow and Duddy, 1981; Harrison, 1985; Green *et al.*, 1985), although this value varies with cooling rate and fluorine/chlorine composition. All of our samples are from igneous rocks that have compositions similar to, or more F rich than Durango apatite, hence the closure temperature for apatites cooling at rates of 1–100°C/m.y. over geological time is taken to be 100 ± 20°C. In a very slow annealing condition (i.e. at temperatures between 120°C and 60 ~ 70°C for a long time), the FT age represents a mixture of tracks through a long time and thus may have no geological meaning (e.g. Green, 1988). Thus an apatite fission track age must therefore be taken as a reflection of both the time over which tracks have been retained and the amount of shortening (annealing) that has taken place, and it represents an integrated measure of that thermal history for an annealed apatite sample. Only when the mean lengths are long (in the range of 14–15 μm), and the cooling history is relatively simple, will the apatite fission track age be interpreted as the time when the sample passed through ~100°C (Green, 1988).

A paleogeothermal gradient of ~30°C/km is assumed in converting cooling histories into unroofing rates. We think ~30°C/km is a reasonable estimate for a geothermal gradient in an orogenic terrane like Tibet (e.g. Blackwell, 1971), though the exact value is impossible to know at present. Such an assumption of paleogeothermal gradient is not required where a correlation between cooling age and elevation exists.

The FT analysis results are summarized in Table 1. Figure 2 is an elevation–age plot of all data, and a general correlation is not found. There is a clustering of ages around 20 Ma. Seven confined track length measurements are shown in Fig. 3. These data are geographically divided into five groups, and are discussed in the following sections in conjunction with previously reported $^{40}Ar/^{39}Ar$ data.

Table 1. Apatite fission track ages

Sample number	Location and lithology	Number of grains	Density of tracks (10^6/cm^2) ρ_d (N_d)	ρ_s (N_s)	ρ_i (N_i)	$P(\chi^2)$ (%)	Age $\pm 1\sigma$	Elevation (m)
Nyainquentanglha–Yangbajain area								
P28-1	NQTL Orthogneiss	40	3.842 (2373)	0.0337 (66)	1.64 (3206)	90	3.6 ± 0.5	4400
P72-1	NQTL Orthogneiss	27	3.803 (2373)	0.0212 (28)	1.11 (1475)	99	3.3 ± 0.6	5100
K56	NQTL Granite	31	4.036 (2373)	0.0759 (76)	2.62 (2622)	99	5.3 ± 0.6	5600
PC56	NQTL Granite	20	4.307 (2373)	0.0809 (69)	3.13 (2665)	90	5.1 ± 0.6	5020
PC29	YBJ Granite	20	4.341 (3231)	0.739 (126)	15.3 (2604)	90	9.5 ± 0.9	4300
W. Majiang area and Maqu area								
K3	MAJANG Dacite	20	4.459 (27270	0.0854 (41)	1.13 (544)	30	15.2 ± 2.5	4400
K53	MAQU Ignimbrite	20	3.977 (2373)	0.179 (52)	0.842 (239)	95	39.3 ± 6.2	≥4150
K33(A)	MAQU Diorite	14	3.881 (2373)	0.161 (81)	0.626 (314)	98	45.2 ± 5.9	3870
K33(B)		12	3.919 (2373)	0.207 (101)	0.781 (381)	70	47.0 ± 5.5	
Nyemo area								
PC11	PARGUCHU Granodiorite	22	4.365 (2716)	0.214 (60)	2.78 (779)	80	15.1 ± 2.1	4600
PC12	PARGUCHU Granodiorite	15	4.301 (3231)	0.186 (70)	2.12 (776)	99	17.1 ± 2.2	4200
PC59	W. QUXU Granite	30	4.230 (2373)	0.208 (158)	5.76 (4368)	50	6.9 ± 0.6	3700
Quxu–Lhasa area								
M369	QUXU Granodiorite	17	4.261 (3231)	0.377 (249)	4.72 (3119)	20	15.4 ± 1.1	4600
M370	QUXU Granodiorite	20	4.221 (3231)	0.432 (269)	4.88 (3179)	80	16.2 ± 1.2	4350
M371	QUXU Granodiorite	10	4.181 (3231)	0.627 (198)	7.46 (2355)	95	15.9 ± 1.3	4100
M372	QUXU Granodiorite	10	4.141 (3231)	0.368 (160)	4.51 (1964)	90	15.3 ± 1.4	3850
M373	QUXU Granodiorite	25	4.191 (2373)	0.929 (388)	11.8 (4923)	80	15.0 ± 0.9	3600
PC30	QUXU Granite	20	4.253 (2727)	0.544 (184)	5.41 (1661)	70	19.4 ± 1.5	3760
PC32	QUXU Granite	20	4.211 (2727)	0.165 (137)	1.74 (1450)	98	18.1 ± 1.7	4560
H1	QUXU Granodiorite	16	4.021 (3231)	0.456 (201)	4.47 (1973)	10	18.6 ± 1.5	3800
H2	QUXU Granodiorite	10	4.583 (2727)	0.564 (208)	5.48 (2021)	1	21.4 ± 2.9*	3600
K73	QUXU Granodiorite	12	4.152 (2373)	0.494 (217)	4.59 (2016)	70	20.2 ± 1.6	3440
PC36	GU-RONG Granite	20	4.061 (3231)	0.581 (206)	5.12 (1818)	50	20.8 ± 1.7	4500
PC39(A)	GU-RONG Granite	21	3.941 (3231)	0.394 (160)	3.54 (1438)	30	19.9 ± 1.8	3750
PC39(B)		12	4.005 (2727)	0.690 (184)	6.23 (1661)	70	20.1 ± 1.7	
K45	LHASA Granite	8	3.764 (2373)	0.255 (41)	1.72 (277)	30	25.2 ± 4.3	3720
Dagze area and Samye area								
K66	DAGZE Granite	10	4.113 (2373)	0.250 (57)	1.40 (271)	50	33.3 ± 5.2	5050
K72	DAGZE Granite	20	3.981 (3231)	0.347 (98)	3.27 (924)	80	19.1 ± 2.1	3975
PC62	SAMYE Tonalite	22	4.280 (2716)	0.301 (89)	2.09 (619)	50	27.5 ± 3.3	4440
PC65	SAMYE Tonalite	20	4.348 (2531)	0.331 (146)	0.61 (1153)	80	24.9 ± 2.3	3750

An EDM method was used for these analyses. (A), (B) after a sample number indicates two independent analyses of the same sample. An asterisk (*) indicates that the mean (ρ_s/ρ_i) was used to calculate age as the sample failed the (χ^2) test at the 5% level. NQTL = Nyainqentanglha Range. YBJ = Yangbajain.

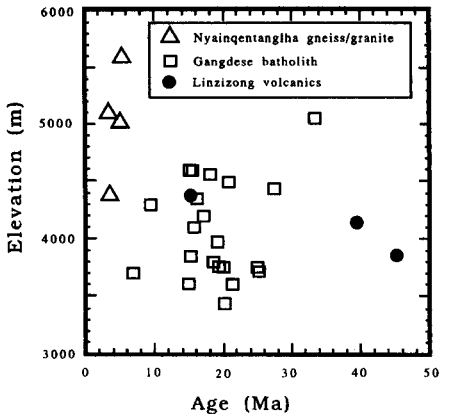

FIG. 2. An FT age–elevation plot of all the apatite samples analyzed. No general correlation exists between age and elevation. Notice there is a clustering of ages around 20 Ma.

3.1. *Yangbajain area*

3.1.1. *Nyainqentanglha Range.* Apatites (P28-1, P72-1, K56, PC56) from the granite rocks and orthogneisses of the Nyainqentanglha range, west of the Yangbajain graben, yield exceptionally young FT ages of between 3.3 ± 0.6 (1 σ standard deviation, the same hereinafter) and 5.3 ± 0.6 Ma. Together with $^{40}Ar/^{39}Ar$ data (Copeland, 1990), cooling rates of 30 to 300°C/m.y. (9–0 Ma) at several locations can be deduced (Table 2), which can be transferred to an unroofing rate of 1–10 mm/y. Such a high rate must have caused upward disturbance of isothermals; therefore, a 30°C/km gradient may be lower than the true value. Even if the gradient was doubled, the unroofing would still be as high as 0.5–5 mm/y. These young ages and fast cooling rates reflect recent rapid uplift and exhumation of the foot-wall of a major normal-faulting detachment zone accompanying the Yangbajain graben (Pan and Kidd, 1992).

3.1.2. *Yangbajain pluton.* Previously, a U–Pb zircon age of 50 Ma, and two Rb–Sr isochron ages of 49.0 and 49.2 Ma have been reported (Xu *et al.*, 1985; Debon *et al.*, 1986) for this pluton. A granodiorite intrusion (PC29) yields an apatite age of 9.5 ± 0.9 Ma. The same sample gives a K-feldspar $^{40}Ar/^{39}Ar$ age spectrum reflecting cooling through ~270°C at around 39 Ma, and a biotite granite from a nearby

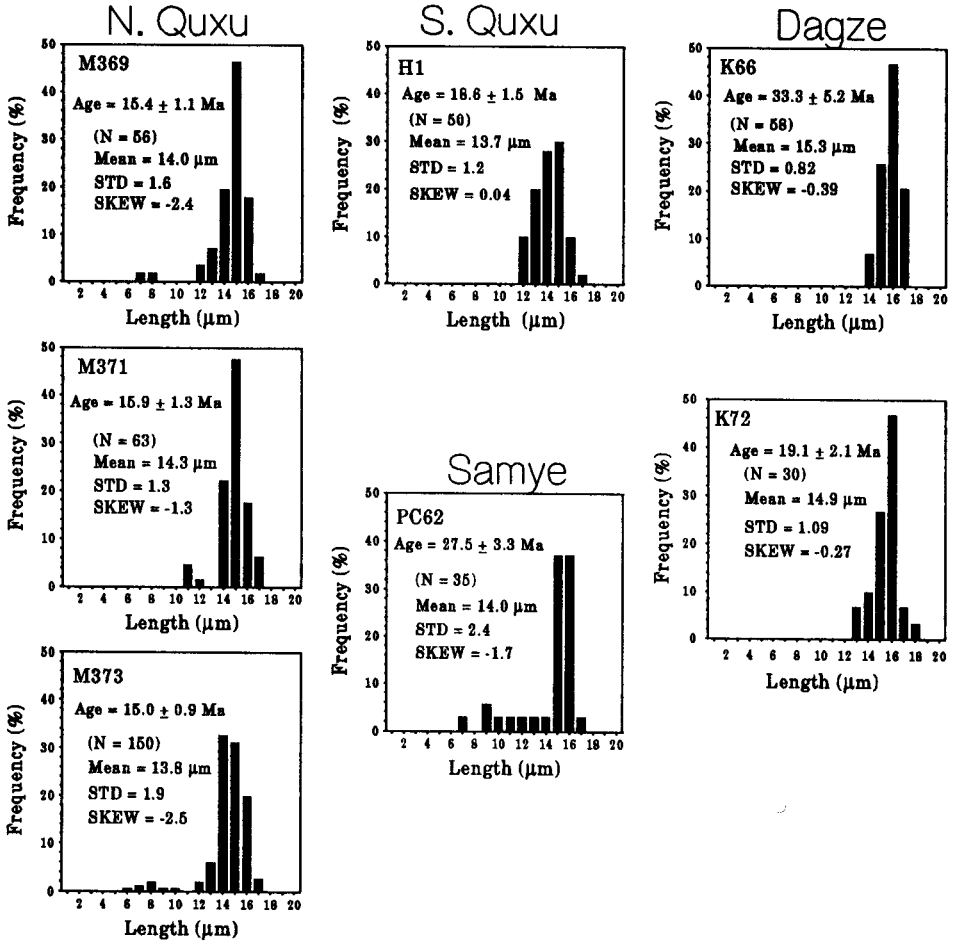

FIG. 3. Confined fission track length distributions from selected samples, including three from the northern Quxu area, one from the southern Quxu area, one from the Samye area, and two from the Dagze area. Listed in each distribution diagram are also the FT age, number of tracks measured (N), mean track length (in microns), standard deviation (STD), and skewness (SKEW).

Table 2. Thermochronology of the Nyainqentanglha Range

Sample location	Mineral/ method	Cooling age (Ma)	Closure temperature (°C)	Cooling rate (°C/m.y.)
North (P72-1)	ksp/Ar–Ar	8.1 ± 0.1	360 ± 15	
	bio/Ar–Ar	6.2 ± 0.1	320 ± 25	21 ± 15
	ksp/Ar–Ar	3.7 ± 0.1	250 ± 15	28 ± 12
	ap/FT	3.3 ± 0.6	100 ± 20	300 ± 300
Central (P28-1)	hbl/Ar–Ar	6.5 ± 0.9	550(?)	
	ksp/Ar–Ar	5.6 ± 0.2	335 ± 15	~239
	ksp/Ar–Ar	4.3 ± 0.2	235 ± 15	77 ± 24
	ap/FT	3.6 ± 0.5	100 ± 20	193 ± 142
South (K56)	mus/Ar–Ar	14.6 ± 0.1	350 ± 25	
	bio/Ar–Ar	13.0 ± 0.1	320 ± 25	19 ± 22
	ksp/Ar–Ar	9.5 ± 0.2	230 ± 15	54 ± 8
	ap/FT	5.3 ± 0.6	100 ± 20	31 ± 7

$^{40}Ar/^{39}Ar$ data of biotite (bio), K-feldspar (ksp) are from Copeland (1990). Apatite (ap) FT data are from this study. All the estimated errors are at the 1 σ level.

location has yielded K-feldspar data that indicate this granite has cooled from 250 to 200°C during 29–20 Ma (Copeland, 1990; Copeland *et al.*, 1993). These data suggest an average cooling rate of ~6°C/m.y. between 39 and 10 Ma and an unroofing rate of 0.2 mm/y. If these data are representative of the whole pluton, then the cooling history from 20 to 10 Ma and 10 Ma to the present can be refined as ~10°C/m.y. and an unroofing rate of 0.3 mm/y can be deduced. Therefore, the average cooling rate of the Yangbajain pluton has increased from ~4°C/m.y. to ~10°C/m.y. since 20 Ma (Fig. 4). This corresponds to an increase in unroofing rate from ~0.1 to ~0.3 mm/y.

3.2. *Western Majiang area and Maqu area*

Both areas are covered by the Cenozoic Linzizong volcanics. The eruption ages of the volcanic rocks in these areas were reported to be 50–60 Ma (Coulon *et al.*, 1986; Pan, 1993). An ignimbrite sample from Maqu (K33) yields an apatite FT age of 39.3 ± 6.2 Ma. A dioritic stock (K33) in the Maqu area coexists with the Linzizong volcanics and it yields a biotite $^{40}Ar/^{39}Ar$ plateau age of 65.0 ± 2.8 Ma (Pan, 1993). Two independent analyses of the apatite from K33 suggest an FT age of ~45 Ma. Pan *et al.* (1991) argued that these volcanic rocks in the Maqu area were deeply buried up to 7 km (at temperature > ~ 180°C) and experienced slow cooling at a rate of 10°C/m.y. between 54 and 44 Ma. The FT age seems to agree with this interpretation but clearly more ages and length distributions are required to draw reliable conclusions.

To the west of Majiang, a dacitic tuff (K3) has yielded an $^{40}Ar/^{39}Ar$ biotite isochron age of 14.9 ± 0.2 Ma (see Pan, 1993 for details). The same sample yields an apatite FT age of 15.1 ± 2.1 Ma, in good agreement with the $^{40}Ar/^{39}Ar$. This result further confirms the Miocene age of the volcanism in this area.

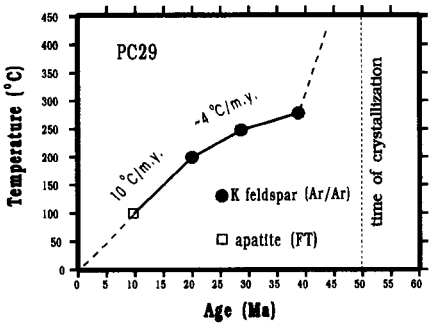

FIG. 4. A closure temperature vs cooling age plot for the Yangbajain pluton (sample PC29). The K-feldspar $^{40}Ar/^{39}Ar$ data are from Copeland *et al.* (1993). These data suggest that the average cooling rates were ~4°C/Ma between 40 and 20 Ma, and ~10°C/Ma since 20 Ma.

3.3. *Nyemo area*

About 18 km northwest to Nyemo, two samples (PC11, PC12) were studied by FT dating, and apatite ages of 15 and 17 Ma were obtained with large errors, owing to the lack of suitable grains. These two ages are negatively correlated with elevation, which was not expected, and this perhaps is a reflection of large errors. Nevertheless, these two ages are still within agreement with $^{40}Ar/^{39}Ar$ biotite and K-feldspar ages of ~15 Ma (Copeland *et al.*, 1993). It is possible that a very rapid cooling event has occurred in this location at ~15 Ma but more thermochronological data are required to confirm this inference.

About 25 km to the east of Nyemo, a weakly foliated microgranite (PC59) yields a FT apatite age of 6.9 ± 0.6 Ma. This age is much younger than most other samples in Quxu area but closer to FT ages in the Nyainqentanglha Range. It is possible that this young age is also related to the east–west extensional tectonics in this general region. No other geochronology data are available from this location.

3.4. *Quxu–Lhasa area*

3.4.1. *Quxu pluton, north.* Copeland *et al.* (1987) have suggested a pulse of accelerated rapid cooling around 19–17 Ma, mainly based on $^{40}Ar/^{39}Ar$ data. Five samples (M369, M370, M371, M372, and M373) with 250 m vertical separation between each sample yield biotite $^{40}Ar/^{39}Ar$ ages that are clearly correlated with elevation, and the slope of the elevation–age curve steepens with decreasing age from 26.8 to 17.8 Ma. Potassium feldspar age spectra of these samples have yielded a common lower plateau of 17.0 at a closure temperature of 285°C (Copeland *et al.*, 1987).

The same set of samples (M369–M373) were used in this study. They yield FT apatite pooled ages of 15–16 Ma, positively correlated with elevation (except for the top one whose pooled age is younger than the middle sample), but indistinguishable from each other within 1 σ error range. The apatite fission track ages and their biotite $^{40}Ar/^{39}Ar$ ages are plotted against elevation in Fig. 5(a), and cooling ages vs closure temperatures for M373 are plotted in Fig. 5(b). These data suggest that cooling of these samples at around 17–15 Ma was rapid, in excess of 80°C/m.y. (Fig. 5(b)).

The above data indicate that the unroofing rate at this location has been less than 0.07 mm/y prior to 23 Ma, then increased to over 0.2 mm/y at around 20 Ma, reached over ~3 mm/y at around 17–15 Ma, and after ~15 Ma the average unroofing rate has been 0.2 mm/y. Therefore, a distinctive pulse of unroofing during 20–15 Ma is revealed.

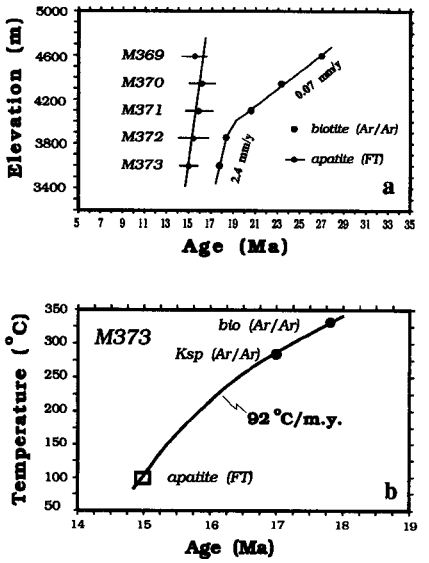

FIG. 5(a). Age–elevation plot of five samples from a granodiorite at north Quxu. Vertical separation between samples is 250 m (±15 m). Both apatite FT ages (with 1 σ error bars) of this study and biotite $^{40}Ar/^{39}Ar$ ages (1 σ range smaller than the symbol) from Copeland *et al.* (1987) are plotted. The correlation between biotite ages and elevations suggest an increase in unroofing rate from 0.07 to 2.4 mm/y at ~19 Ma, and the five apatite FT ages also suggest rapid unroofing at around 15–16 Ma. (b) Temperature–time path for the lowermost sample (M373) based on mineral cooling ages and closure temperatures. An average cooling rate of 92°C/m.y. is obtained, indicating an unroofing rate of over 3 mm/y between 15 and 17 Ma. See text for discussion.

Three FT length distributions from top, middle, and bottom of this traverse were obtained (M369, M371, M373, see Fig. 3). The mean lengths range from 13.8 ± 1.9 to 14.3 ± 1.3 μm. These track length distributions are consistent with a cooling history of initial fast cooling followed by a longer period of slower cooling, probably at the upper part of a partial annealing zone, at temperatures of 60–70°C. Therefore, the track length data from this location are suggestive of slow cooling and unroofing (ca. less than 6°C/m.y. and 0.2 mm/y) after ~15 Ma. Because the average unroofing rate was ~0.2 mm/y since 15 Ma, there was probably another pulse of cooling and unroofing at a more recent time.

3.4.2. *Quxu pluton, central and south.* Two apatite samples with 800 m vertical separation (PC30, PC32) from the central part of the Quxu pluton yield similar ages of 19.4 ± 1.5 and 18.1 ± 1.7 Ma, which can be interpreted to have resulted from rapid cooling at that time. Although there are only two ages, this interpretation is in good agreement with the results of Richter *et al.* (1991), in which accelerated cooling at 20–15 Ma was found to have been experienced by sample PC32.

Apatites from the southern Quxu area (H1 and H2, near the Quxu village, and K73 just south of the Zangbo river) yield FT ages of 19–21 Ma. Sample H1 has yielded $^{40}Ar/^{39}Ar$ biotite and K-feldspar ages indicating cooling between 42 and 30 Ma from 250 to 210°C (Copeland *et al.*, 1993). These data reveal a period of relatively slow cooling from 42 to 19 Ma at a rate of ~10°C/m.y., which corresponds to an unroofing rate of 0.3 mm/y, assuming a geothermal gradient of 30°C/km. An acceleration in the rate of cooling after 19 Ma is not detectable at this location, but sample H1 shows an FT length distribution (Fig. 3) in agreement with a history of rapid cooling at 19–20 Ma to ~60°C, followed by a period of prolonged slow cooling.

3.4.3. *Gu-Rong pluton.* Two apatite samples (PC36, PC39) with 750 m vertical separation from Gu-Rong granite yield FT ages of 20.8 ± 1.7 and 20.0 ± 1.7 Ma (Fig. 6(a)), respectively. The second age is the average of two independent measurements (different irradiations). Hornblende, K-feldspar, and biotite $^{40}Ar/^{39}Ar$ ages have been obtained from the lower sample (Copeland *et al.*, 1993) and they are plotted together with FT ages against their respective closure temperatures (Fig. 6(b)). The average cooling rate between 44 and 20 Ma is ~6°C/m.y., which corresponds to an unroofing rate of 0.2 mm/y. We interpret the essentially identical apatite FT ages with 750 m vertical separation as a consequence of rapid cooling at around 20 Ma.

3.4.4. *Lhasa pluton.* An apatite sample (K45) from the Lhasa granite yields an apatite FT age of

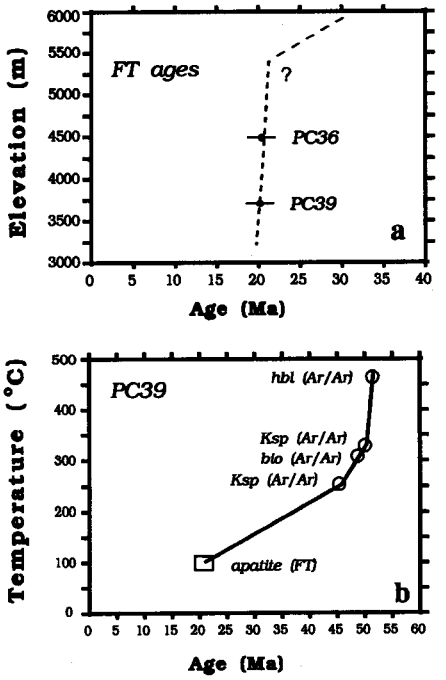

FIG. 6(a). FT age–elevation plot of the two apatites from the Gu-Rong pluton. Vertical separation between the two samples is 750 m. Error bars are at the 1 σ level. The question mark indicates that the position of a "break in slope", if it exists, should be found above 4500 m in this area. (b) Temperature–time path of the lower sample (PC39) based on mineral cooling ages and their closure temperatures. $^{40}Ar/^{39}Ar$ data are from Copeland *et al.* (1993).

~25 Ma. There is a large error associated with this age owing to lack of suitable grains and relatively low U content. This sample has yielded $^{40}Ar/^{39}Ar$ K-feldspar ages ranging from 40–48 Ma with closure temperatures 220–290°C (Copeland *et al.*, 1993). These data suggest an average cooling rate of ~8°C/m.y. between 40 and 25 Ma and an average cooling rate of ~4°C/m.y. since 25 Ma.

3.5. *Dagze area and Samye area*

3.5.1. *Dagze pluton.* Two samples (K72 at 3975 m and K66 at 5050 m) yield FT ages of 19.1 ± 2.1 and 33.3 ± 5.2 Ma, respectively. These two samples yield long mean track length of 14.9 and 15.3 μm, respectively (see Fig. 3). The standard deviation is only 1.1 for the lower sample, and is 0.8 for the upper sample. These two track length distributions suggest that the two samples cooled relatively fast at different time. Therefore, the possibility that these samples came from an uplifted partial annealing zone, such as the one discussed by Fitzgerald and Gleadow (1990), can be ruled out. An unroofing rate of 0.08–0.15 mm/y for the period of 33–19 Ma can be assigned to this pluton (Fig. 7(a)). Potassium feldspar from sample K72 has given an $^{40}Ar/^{39}Ar$ partial plateau age of 40 Ma with a closure temperature 230°C (Copeland *et al.*, 1993). A cooling rate of 6°C/m.y. and an unroofing rate of 0.2 mm/y can be calculated for sample K72 based on these data (Fig. 7(b)). All these data suggest that the unroofing rate at this location was 0.08–0.2 mm/y between 40 and 19 Ma.

3.5.2. *Samye pluton.* Apatite from a tonalite (PC65) gives an FT age of 24.9 ± 2.3 Ma. Another sample from a higher elevation (PC62) yields an older apatite FT age of 27.5 ± 3.3 Ma (Fig. 8(a)). Thirty-five confined track length measurements yield a mean track length of 14 μm (see Fig. 3), which we consider to have resulted from relatively rapid cooling, though the small number of tracks measured precludes definite conclusions. The lower sample has yielded an $^{40}Ar/^{39}Ar$ biotite plateau age of ~48 Ma (Copeland, 1990; Copeland *et al.*, 1993). This suggests that the sample has cooled from ~330 to ~100°C from 48 to 25 Ma with a rate of ~10°C/m.y. (Fig. 8(b)). The average cooling rate after 25 Ma has been only ~4°C/m.y. These data suggest an average unroofing rate of 0.3 mm/y for the period between 48 and 25 Ma and an average unroofing rate of 0.1 mm/y since 25 Ma.

4. DISCUSSION

The FT data from two locations in the northern and central Quxu area reveal that very rapid cooling

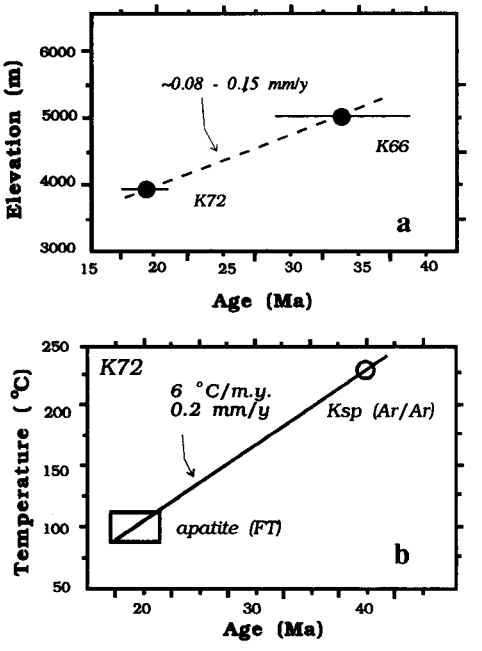

FIG. 7. Age–elevation plot (a) and cooling path (b) of the Dagze granite. Vertical separation between K66 and K72 is 1075 m (±25 m). Both samples have long confined track length (~15 μm, see Fig. 3). Average unroofing rate of 0.08 ~ 0.15 mm/y is calculated by using the slope of the line in (a), which is compatible with the cooling and unroofing rate (6°C/m.y. and ~0.2 mm/y) obtained by using the closure temperature/cooling age approach. $^{40}Ar/^{39}Ar$ data are from Copeland *et al.* (1993).

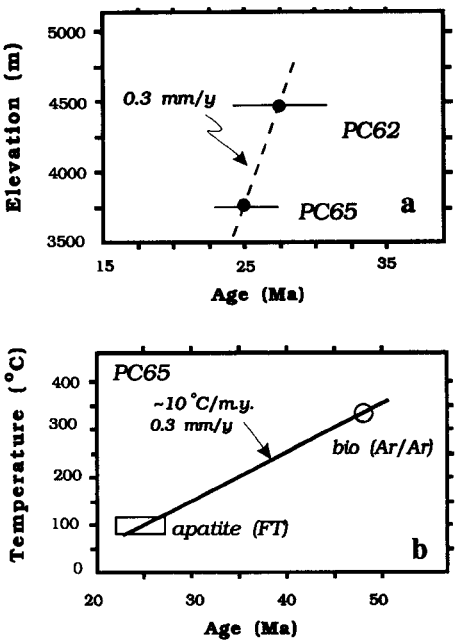

FIG. 8. Age–elevation plot (a) and cooling path (b) of the Samye Tonalite (sample PC62 and PC65). Vertical separation between these two samples is 690 m (±25 m). Average unroofing rate of ~0.3 mm/y is indicated in (a). As the difference in ages is small and only two ages are available, the uncertainty may be large. However, this rate is the same as that obtained in (b), by using the closure temperature/cooling age approach. $^{40}Ar/^{39}Ar$ data are from Copeland *et al.* (1993).

(over 80°C/m.y.) occurred between ~20 and ~15 Ma. Data from the southern Quxu area (near Quxu village) reveal a slow cooling period from 42 to 19 Ma at a rate of ~10°C/m.y. Accelerated cooling after 19 Ma is not detectable here, but one of the samples shows an FT length distribution consistent with a history of rapid cooling at 19–20 Ma from > ~110°C down to ~60°C, followed by a period of prolonged slow cooling to the surface temperature. Data from the Yangbajain granite also indicate that the unroofing rate has increased since 20 Ma, from about 0.1 to 0.3 mm/y. These data therefore support the view that the cooling and unroofing in the Quxu area were accelerated at around 20 Ma (Copeland *et al.*, 1987; Richter *et al.*, 1991). This accelerated cooling can be detected in the Quxu pluton complex along the Quxu–Lhasa traverse, in the Gu-Rong granite to the west of Lhasa, and possibly in the Yangbajain granite. Average cooling rates of 4–9°C/m.y. (45–0 Ma) are obtained for all these locations, which can be translated to unroofing rates of 0.1–0.3 mm/y. These relatively low rates can be viewed as a regional "background" in this mountain-building area, and the rapid cooling in the Quxu and Gu-Rong areas as a "pulse" superimposed on it.

Apatite FT data and $^{40}Ar/^{39}Ar$ data from Samye area and Dagze area suggest slow cooling and unroofing rates (0.1–0.3 mm/y) in these places. Though these data do not suggest a pulse of rapid cooling and unroofing has occurred in these areas, they do not automatically exclude it. For example, it is conceivable that the present surface rocks from these areas have been rapidly brought to the surface by the same pulse of unroofing experienced in the rocks to the west, and have been subsequently sitting there for a long time because of the later low unroofing rate.

Rapid cooling and unroofing recorded in rocks from the Quxu–Lhasa area at around 20–15 Ma may not be restricted to this region and several lines of evidence for a regional event have been summarized by Harrison *et al.* (1992). These include the thick Miocene molasse sediments south of Himalaya (e.g. Johnson *et al.*, 1985), the erosion record seen from detrital minerals from the Siwalik sandstone, the modern Zangbo River, and the Bengal fan (e.g. Cerveny *et al.*, 1988; Copeland and Harrison, 1990; Corrigan and Crowley, 1990), and unroofing studies in western Himalaya (Zeitler, 1985). In addition to those lines of evidence discussed by Harrison *et al.* (1992), Sorkhabi (1994) found that there is a clustering of apatite ages of 20–25 Ma from the Trans-Himalaya batholith in Ladakh region of northwestern India (about 1000 km west–northwest extension of the Quxu–Lhasa area), and between 20–25 Ma (apatite FT ages) and 41–45 Ma (zircon FT ages) the average cooling rate is only about 4.5°C/m.y. Lewis (1990) reported apatite FT ages of 19–20 Ma in the central–eastern Kunlun range of the north margin of Tibet, south of Golmud City, which may be interpreted as onset of uplift (to the surface) at 20 Ma or later. There are thick Neogene molasse deposits along the north, south, and east margins of the Tibetan plateau (e.g. Fatmai, 1974; Hsü, 1988; Chang *et al.*, 1989), and there are also very thick Miocene sediments in the Bengal fan in the Indian Ocean (see Stowe *et al.*, 1989), suggesting fast unroofing of Tibet and Himalaya since ~20 Ma. Thus, our data together with all these data tend to indicate that the unroofing was abruptly intensified around 20 Ma in southern Tibet. If this rapid unroofing event in southern Tibet was a consequence of elevated topography, then the uplift history of Tibet may have been episodic and non-steady. It follows that southern Tibet did not respond to the collision immediately, therefore some of these proposed tectonic hypotheses such as underplating, and hydraulic injection are not favored. Following the thoughts of Molnar and England (1990), one may interpret the abrupt intensification of unroofing in southern Tibet and dumping of sediments to its surroundings as a consequence of a dramatic climatic change at that time. While there is no evidence for such a scenario, there are two clues, though themselves interpretations, that support the uplift and erosion view: (1) the gravitational collapse represented by the High Himalaya detachment system (Burg *et al.*, 1984; Burchfiel and Roydon, 1985) was active just prior to 20 Ma (Hodges *et al.*, 1991), indicating that the

elevation of this area was already significant; (2) eastward continental escape of Tibetan plateau since collision has taken place along large-scale strike–slip faults such as the Red River Fault (Tapponnier *et al.*, 1986), during 35 to 19–20 Ma (Leloup and Harrison, 1992). After 20 Ma the collisional convergence may have been taken by thickening in Tibet, as expressed by the cooling and unroofing history of the Quxu–Lhasa area. We favor the explanation of uplift (thickening)-erosion, over that of climate change-erosion, but definite evidence is not yet available. Future geological and thermochronological studies themselves may provide the answer to this question, because climate change does not require geological processes right underneath the rapidly cooled sample location but tectonic uplift via vertical straining does. For example, if all spatially separated locations that experienced the same rapid unroofing can be associated with crustal thickening processes such as faulting and folding, then climate change scenarios would not be valid.

The very young and rapid cooling and unroofing in the Nyainqentanglha range is clearly related to extension in this region (Pan and Kidd, 1992), and therefore we consider these cooling ages not to be related to uplift relative to sea level. The ultimate result of lateral extension would result in lowering, rather than uplift, of the surface of Tibet. We want to emphasize that both the geological and geomorphic setting should be considered when interpreting thermochronological data. The sample PC59 is an example of this, the relatively young FT apatite age (6.9 ± 0.6 Ma) may be related to normal faulting associated with the Yangbajain rift system, or alternatively related to the southward thrusting along the suture line (see Allègre *et al.*, 1984). The geology at that location is not adequately known to confirm these speculations.

5. SUMMARY

FT analysis support the previous view that the north Quxu pluton has experienced a pulse of rapid cooling (>80°C/m.y.) and unroofing (>2 mm/y) around 20–15 Ma, in contrast to the average background cooling rate of 4–10°C/m.y. and unroofing rate of 0.1–0.3 mm/y. This rapid cooling event has also been detected to have existed to north and south of this location, in the Gu-Rong pluton and central–south Quxu pluton.

Such a pulse of rapid unroofing event may have been prevalent in Tibet, which may be interpreted as a result of intensified crustal thickening and resulted surface uplift at that time. If this is true, the crustal thickening and uplift history of southern Tibet would have been non-steady and a profound acceleration would have occurred some 20 Ma after the initial collision at ~45 Ma between India and Asia. Some of the proposed uplift models that predict steady processes and early response of southern Tibet to the India–Asia collision, such as continental underthrusting and continental injection, are not favored by these data.

FT apatite ages of the Nyainqentanglha are as young as 3.3 ± 0.6 Ma and they are interpreted as a result of tectonic unroofing via a low-angle extensional detachment zone present at the southeast margin of the range. Therefore they do not represent crustal thickening and surface uplift of the Tibetan plateau.

Acknowledgements—Zhang Yuquan, Xie Yinwei, and Zhu Bingquan, all from the Institute of Geochemistry in Guiyang, China, are thanked for their assistance in the field work and sample collection. Our successful field work in Tibet would have been impossible without their well-made preparation and organization. We have benefited from discussion with D. S. Miller and C. E. Ravenhurst, both from R.P.I. We also wish to acknowledge two anonymous reviewers for detailed and constructive criticisms of the original manuscript. The work presented in this paper was supported by an NSF grant (EAR 87-21026) from the tectonics program to W. S. F. Kidd.

REFERENCES

Allègre C. J. and 34 others (1984) Structure and evolution of the Himalayan–Tibet orogenic belt. *Nature* **307,** 17–22.

Blackwell D. D. (1971) The thermal structure of the continental crust. In *The Structural and Physical Properties of the Earth's Crust* (Edited by Heacock, J. G.). *A.G.U. Monogr. Ser.* **14,** 169–184.

Burchfiel B. C. and Royden L. H. (1985) North–south extension within the convergent Himalayan region. *Geology* **13,** 679–682.

Burg J. P., Brunel M., Gapais D., Chen G. M. and Liu G. H. (1984) Deformation of leucogranites of the crystalline main central thrust sheet in southern Tibet (China). *J. Struc. Geol.* **6,** 535–542.

Cerveny P. F., Naeser N. D., Zeitler P. K., Naeser C. W. and Johnson N. M. (1988) History of uplift and relief of the Himalaya during the past 18 million years: evidence from fission-track ages of detrital zircons from sandstones of the Siwalik group. In *New Perspectives in Basin Analysis* (Edited by Kleinspehn K. L. and Paola C.), pp. 43–62. Springer, New York.

Chang C., Pan Y. and Sun Y. (1989) The tectonic evolution of the Qinghai–Tibet Plateau: a review. In *Tectonic Evolution of the Tethyan Region* (Edited by Sengör A. M. C.), pp. 415–476, NATO ASI series C. Kluwer, Dordrecht and Boston.

Copeland P. (1990) Cenozoic tectonic history of the southern Tibetan plateau and eastern Himalaya: evidence from $^{40}Ar/^{39}Ar$ dating, Ph.D. dissertation, State University of New York at Albany, p. 414.

Copeland P., Pan Y., Harrison T. M., Kidd W. S. F., Roden M. K., Zhu Bingquan, Zhang Yuquan and Xie Yingwen (1993) Thermal evolution of the Gangdese Batholith, southern Tibet: a history of episodic unroofing (manuscript submitted to *Tectonics*).

Copeland P., Harrison T. M., Kidd W. S. F., Xu Ronghua and Zhang Yuquan (1987) Rapid early Miocene acceleration of uplift in the Gangdese Belt, Xizang–southern Tibet, and its bearing on accommodation mechanisms of the India–Asia collision. *Earth planet. Sci. Lett.* **86,** 240–252.

Copeland P. and Harrison T. M. (1990) Episodic rapid uplift in the Himalaya revealed by $^{40}Ar/^{39}Ar$ analysis of detrital K-feldspar and muscovite, Bengal fan. *Geology* **18,** 354–357.

Corrigan J. F. and Crowley K. D. (1990) Fission-track analysis of detrital apatites from sites 717 and 718, Leg 116, Central Indian Ocean. In *Proc. ODP, Sci. Results* **116,** 75–92. College Station, Texas (Ocean Drilling Program).

Coulon C., Maluski H., Bollinger C. and Wang S. (1986) Mesozoic and Cenozoic volcanic rocks from central and southern Tibet: 39Ar–40Ar dating, petrological characteristics and geodynamical significance. *Earth planet. Sci. Lett.* **79,** 281–302.

Debon F., Le Fort P., Sheppard S. M. F. and Sonet J. (1986) The four plutonic belts of the Transhimalaya–Himalaya: a chemical mineralogical, isotopic, and chronological synthesis along a Tibet–Nepal section. *J. Petrol.* **21,** 219–250.

Dewey J. F. and Burke K. (1973) Tibetan, Variscan and Precambrian basement reactivation: products of continental collision. *J. Geol.* **81,** 683–692.

Dewey J. F., Shackelton R. M., Chang Chengfa and Sun Yijin (1988) The tectonic evolution of the Tibetan Plateau. *Phil. Trans. R. Soc. Lond.* **A327,** 379–413.

England P. C. and Houseman G. A. (1988) The mechanics of the Tibetan Plateau. *Phil. Trans. R. Soc. Lond.* **A326,** 301–320.

Fatmai A. N. (1974) Lithostratigraphic units of Kohat Potwar Province, Indus Basin, Pakistan. *Geological Survey Pakistan Memoir* **10,** 80.

Fitzgerald P. G. and Gleadow A. J. W. (1990) New approaches in fission track geochronology as a tectonic tool: examples from the Transantarctic Mountains. *Nucl. Tracks Radiat. Meas.* **17,** 351–357.

Gansser A. (1981) The geodynamic history of the Himalaya. In *Zagros, Hindu Kush, Himalaya Geodynamic Evolution* (Edited by Gupta H. K. and Delany F. M.). *Geodynamics Ser.* **3,** 111–121.

Gleadow A. J. W. and Duddy I. R. (1981) A natural long-term annealing experiment for apatite. *Nucl. Tracks Radiat. Meas.* **5,** 169–174.

Green P. F. (1981) A new look at statistics in fission-track dating. *Nucl. Tracks Radiat. Meas.* **5,** 77–86.

Green P. F. (1986) On the thermo-tectonic evolution of northern England: evidence from fission track analysis. *Geol. Mag.* **123,** 493–506.

Green P. F. (1988) The relationship between track shortening and fission track age reduction in apatite: combined influences of inherent instability, annealing anisotropy, length bias and system calibration. *Earth planet. Sci. Lett.* **89,** 335–352.

Green P. F., Duddy I. R., Gleadow A. J. W., Tingate P. R. and Laslett G. M. (1985) Fission track annealing in apatite: track length measurements and the form of the Arrhenius plot. *Nucl. Tracks Radiat. Meas.* **10,** 323–328.

Harris N. B. W., Holland T. B. J. and Tindle A. G. (1988) Metamorphic rocks of the 1985 Tibet Geotraverse, Lhasa to Golmud. *Phil. Trans. R. Soc. London* **A327,** 145–168.

Harrison T. M. (1985) A reassessment of fission-track annealing behavior in apatite. *Nucl. Tracks Radiat. Meas.* **10,** 329–333.

Harrison T. M., Copeland P., Kidd W. S. F. and Tin A. (1992) Raising Tibet. *Science* **255,** 1663–1670.

Hodges K., Burchfiel B. C., Chen Z., Housh T., Lux D., Parrish R. and Royden L. H. (1991) Rapid early Miocene tectonic unroofing of the metamorphic core of the Himalaya: evidence from the Qomolangma (Everest) region, Tibet. *Geol. Soc. Am. Abstr. Programs* **23,** A327.

Hsü J. (1988) Relic back-arc basins: principles of recognition and possible new examples from China. In *New Perspectives in Basin Analysis* (Edited by Kleinspehn K. L. and Paola C.), pp. 245–264. Springer, New York.

Hurford A. J. and Green P. F. (1983) The zeta age calibration of fission-track dating. *Isotope Geosci.* **1,** 285–317.

Johnson N. M., Stix J., Tauxe L., Cerveny P. F. and Tahirkheli R. A. K. (1985) Palaeomagnetic chronology, fluvial processes and tectonic implications of the Siwalik deposits near Chinji Village, Pakistan. *J. Geol.* **93,** 27–40.

Kidd W. S. F., Pan Yunsheng, Chang Chengfa, Coward M. P., Dewey J. F., Gansser A., Molnar P., Shackleton R. M. and Sun Yiyin (1988) Geological mapping of the 1985 Chinese–British (Xizang–Qinghai) Geotraverse route. *Phil. Trans. R. Soc. Lond.* **A327,** 287–305.

Leloup P. H. and Harrison T. M. (1992) Structural petrological and thermal evolution of the Diancang Shan (PRC). *Eos. Trans. AGU Spring Meeting Suppl.* **73(14),** 310.

Lewis C. L. E. (1990) Thermal history of the Kunlun Batholith, N. Tibet, and implications for uplift of the Tibetan Plateau. *Nucl. Tracks Radiat. Meas.* **17,** 301–307.

Molnar P. and England P. (1990) Late Cenozoic uplift of mountain ranges and global climate change: chicken or egg? *Nature* **346,** 29–34.

Molnar P. and Tapponnier P. (1975) Cenozoic tectonics of Asia: effects of a continental collision. *Science* **189,** 419–426.

Naeser C. W. (1981) The fading of fission-track in the geologic environment—data from deep drill holes. *Nucl. Tracks Radiat. Meas.* **5,** 248–250.

Naeser C. W. and Faul H. (1969) Fission-track annealing in apatite and sphene. *J. Geophys. Res.* **74,** 705–710.

Pan Y. and Kidd W. S. F. (1992) Nyainqentanglha shear zone: a late Miocene extensional detachment in the southern Tibet Plateau. *Geology* **20,** 775–778.

Pan Y., Kidd W. S. F., Harrison T. M. and Copeland P. (1991) $^{40}Ar/^{39}Ar$ Thermochronology of Linzizhong Volcanics and timing of deformation in Takena Formation, Southern Tibet. *Eos. Trans. AGU Spring Meeting Suppl.* **72(17),** 288.

Pan Y. (1993) Unroofing history and structural evolution of the southern Lhasa Terrane, Tibetan Plateau: implications for the continental collision between India and Asia, Ph.D. dissertation, State University of New York at Albany, p. 330.

Powell C. McA. and Conaghan P. J. (1975) Tectonic models of the Tibetan plateau. *Geology* **3,** 727–731.

Powell C. McA. (1986) Continental underplating model for the rise of the Tibetan plateau. *Earth planet. Sci. Lett.* **81,** 79–94.

Richter F. M., Lovera O. M., Harrison T. M. and Copeland P. (1991) Tibetan tectonics from $^{40}Ar/^{39}Ar$ analysis of a single K-feldspar sample. *Earth planet. Sci. Lett.* **105,** 266–278.

Schärer U., Xu R.-H. and Allègre C. J. (1984) U–Pb geochronology of Gangdese (Transhimalaya) plutonism in the Lhasa–Xigaze region, Tibet. *Earth planet. Sci. Lett.* **69,** 311–320.

Sorkhabi R. B. (1993) Time–temperature pathways of the Higher Himalayan Crystalline and the Transhimalayan Batholith: a comparison of fission track ages. *Nucl. Tracks Radiat. Meas.* **21,** 535–542.

Stowe D. A. V., Cochran J. R. and ODP Leg 116 Shipboard Party (1989) The Bengal fan: some preliminary results from ODP drilling. *Geomarine Lett.* **9,** 1–10.

Tapponnier P., Peltzer G. and Armijo R. (1986) On the echanics of the collision between India and Asia. In *Collision Tectonics* (Edited by Coward M. P. and Ries A. C.). *Geol. Soc. Spec. Paper* **19,** 115–157.

Wagner G. A. (1968) Fission-track dating of apatites. *Earth planet. Sci. Lett.* **4,** 411–415.

Xu R.-H., Schärer U. and Allègre C. J. (1985) Magmatism and metamorphism in the Lhasa block (Tibet): a geochronological study. *J. Geol.* **93,** 41–57.

Zeitler P. K. (1985) Cooling history of the NW Himalayas. *Tectonics* **4,** 127–151.

Zhao W. L. and Morgan W. J. (1987) Injection of Indian crust into Tibetan lower crust: a two-dimensional finite element model study. *Tectonics* **6,** 489–504.